5-3　28GHz 帯 5G システムの電波ばく露レベルモニタリングと深層学習技術のモニタリング分野への応用

5-3　EMF Exposure Monitoring of 28-GHz-Band 5G Systems and Applications of Deep Learning Techniques in the Field of EMF Exposure Monitoring

劉 森　大西 輝夫　多氣 昌生　渡辺 聡一
LIU Sen, ONISHI Teruo, TAKI Masao, and WATANABE Soichi

第 5 世代（5G）携帯電話システムでは、従来の携帯電話では使用されていなかった高い周波数帯の 28 GHz 帯も使用している。したがって、実環境で 28 GHz 帯の電波ばく露レベルを把握することは重要である。そこで、電波ばく露レベルモニタリングプロジェクトの一環として 28 GHz 帯の電波ばく露レベル評価の検討を行った。本稿では、まず 28 GHz 帯のローカル 5G 基地局の電波ばく露測定について報告する。一方、測定には多大なリソースが必要であり、深層学習、特に人工ニューラルネットワーク（ANN）を用いることにより、電波ばく露レベルを短時間で推定可能となることが期待できる。筆者は、電波ばく露レベル分布を正確かつ効率的に予測するための ANN モデルを提案し有効性の検証を行ったので報告する。

The 5th-generation (5G) mobile phone system uses the 28 GHz band frequency spectrum that has never before been used in conventional cellular phone systems. Therefore, it is important to understand the electromagnetic field (EMF) exposure level in the 28 GHz band resulting from the system in real-world environments. As part of the research project of Acquisition, Accumulation, and Applications of EMF Exposure Monitoring Data, the EMF exposure level in 28 GHz band was evaluated. This paper first discusses the EMF exposure measurement of 28-GHz-band local 5G (L5G) base stations. On the other hand, significant resources are required for these measurements, and by using deep learning techniques, particularly artificial neural networks (ANNs), EMF exposure levels are expected to be estimated efficiently. The author thus has proposed an ANN model for predicting the EMF exposure level distribution accurately and efficiently and reports on its effectiveness.

1 Introduction

Grasping the electromagnetic field (EMF) exposure level in real living scenarios is a key step towards ensuring environmental and occupational health. Financially supported by the Ministry of Internal Affairs and Communications (MIC), as part of our monitoring project, we have conducted a series of measurements [1][2] for that purpose. Currently, fifth-generation (5G) wireless communication is paving its way under the promise of providing society with unprecedented services [3] including enhanced mobile broadband (eMBB), ultrareliable low-latency communication (URLLC), and massive machine-type communication (mMTC). To that end, 5G, for the first time in the history of cellular communications, is deployed at two frequency bands including frequency range 1 (FR1: sub-6GHz) and FR2 (sub-millimeter-wave or millimeter-wave band) and employs advanced techniques in the physical layer including beamforming and massive multiple input multiple output (mMIMO). Beamforming [4] refers to generating a radiating beam that points to a target user at a specific location with respect to the base station (BS) in order to largely mitigate the interference between users and overcome severe radio-wave propagation path loss. mMIMO [5] denotes large-scale MIMO techniques to significantly improve the capacity and throughput of the system. All these certainly strengthen the necessity of grasping the EMF exposure level from 5G systems, especially 5G FR2 systems that employ sub-millimeter-waves or millimeter-waves. Therefore, many on-site measurements

near 28-GHz-band 5G FR2 BSs have been conducted by research groups from all over the world [6]–[11]. Our measurement results are summarized in Section 2. On the other hand, the many measurements that have been conducted motivate the research society to explore possible approaches to efficiently predict the EMF exposure level to overcome the heavy resource consumption of performing on-site measurements. The EMF exposure level is fully dependent on the environment itself, including the geometry, material, and electromagnetic (EM) source. With advanced numerical approaches (e.g., ray tracing [12], finite difference time domain (FDTD) [13], etc.), one can accurately obtain the EMF exposure level of the scenario under test. However, it is still inefficient, as the computational time could be hours for a large-scale scenario. As an important branch of machine learning and deep learning, artificial neural networks (ANNs) have attracted considerable attention in recent years and have achieved tremendous success in many domains such as physics, biochemistry, and social sciences [14]–[15]. With an appropriate network architecture, an ANN model can not only accurately capture the general pattern hiding within the training data but also be generalized to new data that have never been "seen".

Table 1　BS information (non-standalone)

Frequency	28.2 – 28.3 GHz (bandwidth: 100 MHz)
Subcarrier spacing	120 kHz
Number of synchronization beams	64

The most appealing feature is that the model can efficiently yield prediction results once it is trained, usually much faster than conventional numerical approaches. Therefore, with the final goal of generalizing to 28-GHz-band 5G systems in mind, the author has preliminarily developed an ANN model for predicting the EMF exposure level resulting from a dipole antenna operating at 28 GHz. This is discussed in Section 3. EMF exposure monitoring and machine learning will be inseparable in the future, giving rise to a new branch of research. The future prospect is discussed in Section 4.

2 EMF Exposure Monitoring of 28-GHz-Band 5G Systems [16]

2.1 Monitoring approach

On-site measurements were conducted in the vicinity of a 28-GHz-band local 5G (L5G) BS deployed on the campus of Tokyo Metropolitan University in Tokyo, Japan. Here, L5G [17] is a 5G system unique to Japan and is specially designed for a local area such as a university or a factory. The information of the BS is summarized in Table 1. Figure 1 shows the measurement site. The BS is deployed on the roof of a research building at a height of around 25 meters from the ground and is facing the open area in front of the building. A receiving antenna is placed at a distance of around 35 meters away from the BS and is connected to a portable spectrum analyzer (Anritsu MS2090A) to measure the strength of the electric field (E-field) resulting from the BS. The antenna height is 1.5

Table 2　Configurations of measurement sets

Measurement Set	Antenna	Smartphone position and distance both relative to the antenna
Set-1	Horn[1] (gain: 14.4 dBi)	Back (0.5 m)
Set-2	Omni[2] (gain: 1.7 dBi)	Back (0.5 m)
Set-3	Omni[2] (gain: 1.7 dBi)	Back (2.0 m)

[1]Horn: DRH50 (RFspin)
[2]Omni: 01S1165-00 (Waka Manufacturing)

Table 3　Traffic condition for every sub-measurement

Name	Traffic condition	Data rate [Mbps]
Power off	The smartphone is powered off	-
Power on	The smartphone is powered on but without data traffic (no traffic)	-
iPerf3-DL	The smartphone is continuously running the iPerf3* service in the download direction	500 (max)
iPerf3-UL	The smartphone is continuously running the iPerf3* service in the upload direction	20–40

*iPerf3: a tool for generating synthetic traffic between the smartphone and the BS.

meters from the ground. A 5G smartphone is placed in the vicinity of the receiving antenna to ensure the radiating beam of the BS points in the direction of the receiving antenna. There are three sets of measurements in different configurations, as listed in Table 2. The smartphone is placed behind the antenna for all the measurement sets. The smartphone, once powered on, will always have some transmitted power and thus could affect the measurement results. On the one hand, as the horn antenna has a directional radiation pattern, such an effect is easily blocked. On the other hand, for measurement sets using the omni antenna (Sets 2 and 3), different distances between the smartphone and the antenna are adopted to investigate this effect. In addition, there are four sub-measurements with each one having a different data traffic condition for each measurement set. These data traffic conditions are listed in Table 3. For every sub-measurement, the measurement time is 1 min. The settings of the spectrum analyzer are summarized in Table 4.

Table 4　Spectrum analyzer (Anritsu MS2090A) settings

Frequency range	28.2 – 28.3 GHz
Resolution bandwidth (RBW)	1 MHz
Video bandwidth (VBW)	0.01 MHz
Points	101
Sweep time	≈ 6 ms

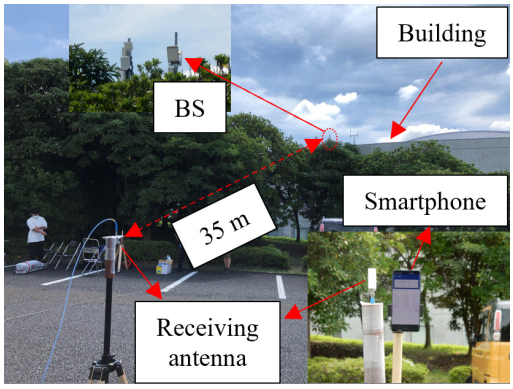

Fig. 1　Measurement site

2.2　Monitoring results

Figures 2 (a) and (b) depict the root mean square (RMS) and maximum (both over 1 min) E-field strengths for every traffic condition in every measurement set, respectively. For each measurement set, the maximum values show little difference between Power on, iPerf3-DL, and iPerf3-UL cases. The RMS E-field strength differences between the iPerf3-DL case and the Power on case are about 24 dB, 19 dB, and 24 dB for Set-1, Set-2, and Set-3, respectively. For all measurement sets, the RMS E-field strengths follow the same trend of iPerf3-DL > iPerf3-UL > Power on > Power off.

Figures 3 (a), (b), and (c) depict the cumulative distribution functions (CDFs) of the instantaneous E-field values for every measurement set, respectively. For all the iPerf3-DL cases shown in Fig. 3, the E-field strengths that correspond to the rapid increases (blue dashed lines) are almost the same, indicating that the E-field strengths purely resulting from the BS are the same. However, there is a gradient-changing region, as marked in Fig. 3 (b). This is caused by the smartphone itself. It is evident that the BS is not continuously transmitting power during the entire measurement duration of iPerf3-UL cases since a significant part of the E-field strength data for this traffic condition is less than the noise threshold marked in Fig. 3 (≈ 60 dBμV/m for Set-1 and 70 dBμV/m for Set-2 and Set-3). Note that the noise thresholds are different since the antennas have different gains.

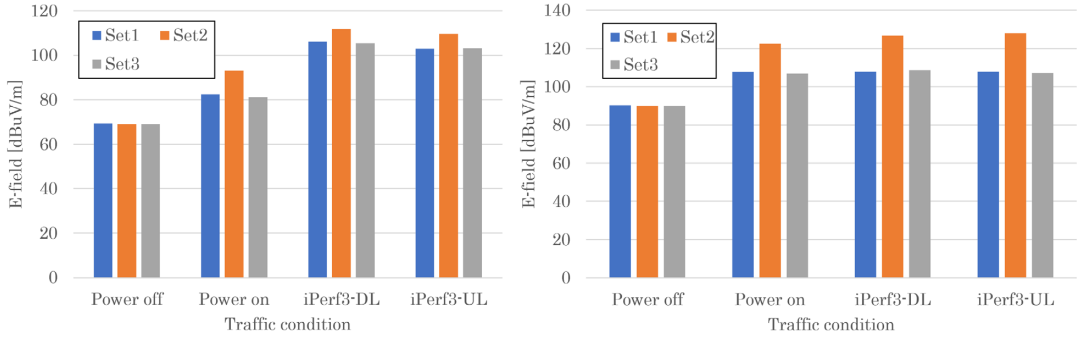

Fig. 2　(a) RMS E-field and (b) maximum E-field strength results over 1 minute

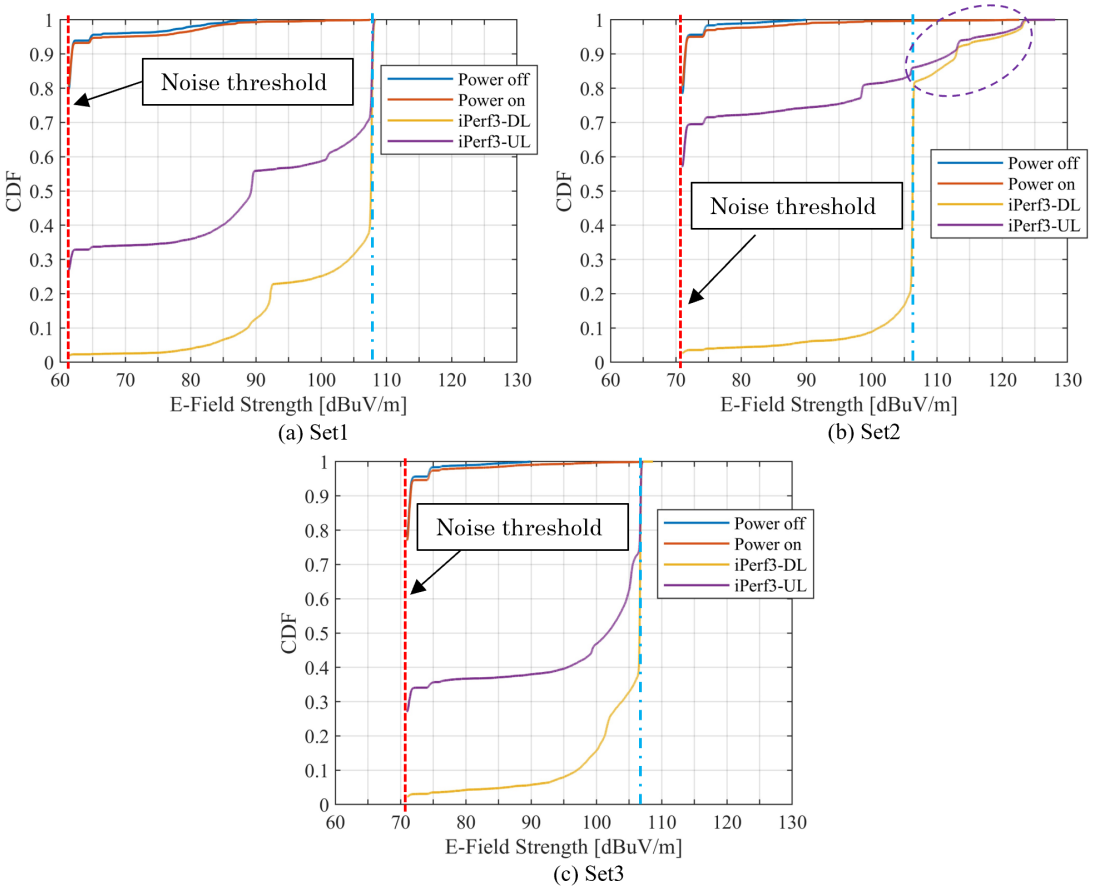

Fig. 3　CDFs for (a) Set-1, (b) Set-2, and (c) Set-3

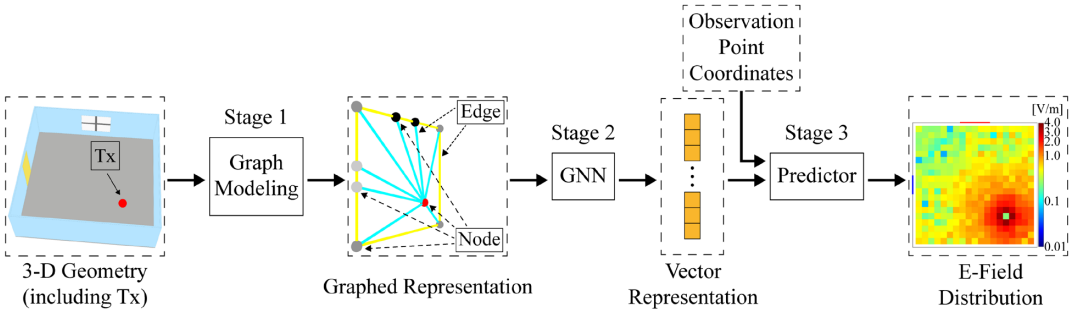

Fig. 4　Prediction model at the top level

3 Applications of Deep Learning Techniques in the Field of EMF Exposure Monitoring [18]–[19]

3.1 Architecture and model

The existing monitoring approaches are usually based on on-site measurements and thus suffer from heavy resource consumption. Aiming at solving this problem, the author has developed a machine learning model for accurately and efficiently predicting the EMF exposure level. The purpose of a machine learning model is to capture the underlying general pattern, in this case, the physics of radio-wave propagations, through learning from the training data. To this end, the input needs to be represented in an appropriate manner so that all the features hidden inside the training data are covered. EMF exposure levels are fully dependent on the environment and the EM source. The authors innovatively represent the environment together with the EM source as a graph, and creatively employs graph neural networks [15][20]. A graph is composed of nodes and edges that connect between nodes and can be well organized to include all the features including the geometry and materials of the environment and the information of the EM source. The overall prediction model is

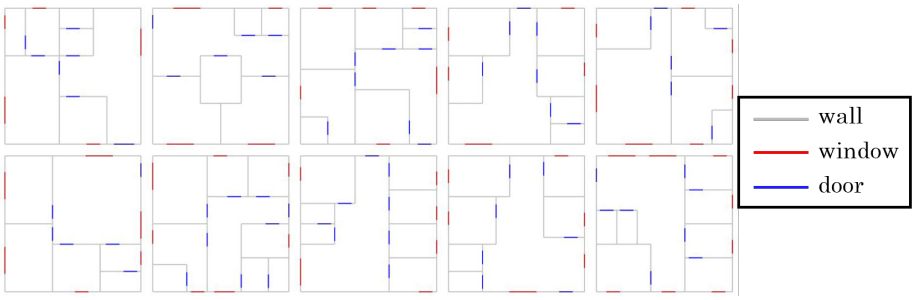

Fig. 5　Some floorplans in the dataset

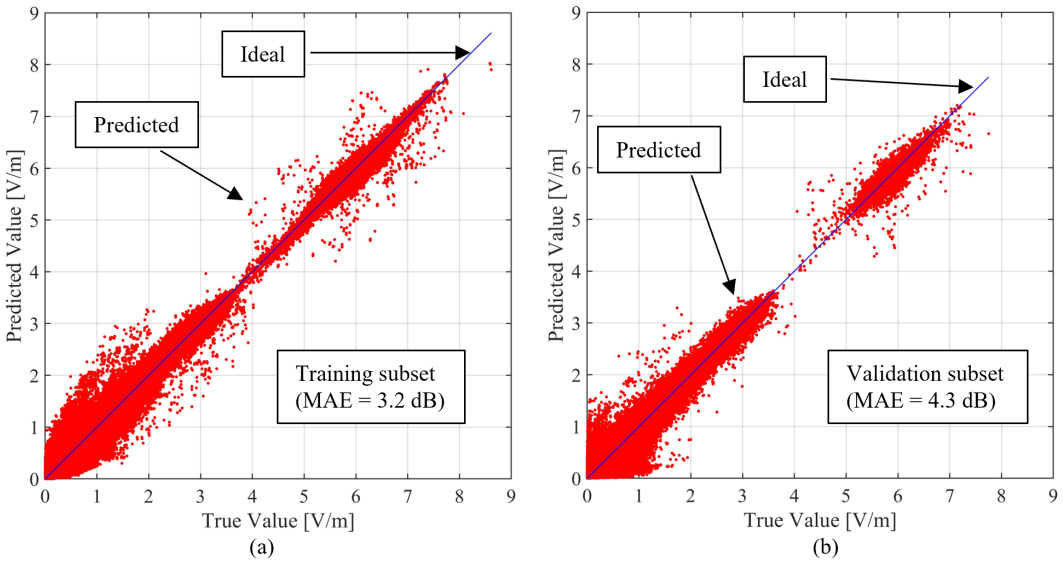

Fig. 6　Scattering plots for the (a) training subset and (b) validation subset

shown in Fig. 4. A given 3-D geometry of the environment including the transmitter (Tx) is first modeled to its graph representation in Stage 1 (Graph Modeling). This graph representation is then used as the input to a graph neural network (GNN) (Stage 2), and is encoded as a vector representation with all the information (environment and EM source) being implicitly included. Finally, the E-field distribution is generated using a predictor network (Stage 3) with the vector representation as input. Here, the predictor is a fully connected neural network.

3.2　Results

Focusing on indoor environments, the author randomly designed one hundred different indoor floorplans (some of the floorplans are shown in Fig. 5) and split them into a training subset (90 floorplans) and a validation subset (10 floorplans). Here, the training subset was used to guide model training, whereas the validation subset was used to test the performance of the trained model. For every floorplan, a dipole antenna operating at 28 GHz was sequentially placed at 180 positions uniformly distributed across that floorplan. Wireless InSite (REMCOM Inc., USA) software was used to calculate the RMS E-field strength distribution, and these data were used as ground truths. The evaluation metric used for quantifying the performance of the prediction model was the mean absolute error (MAE) in dB. The formula is

$$\mathrm{MAE\ [dB]} = \frac{1}{A \cdot K} \cdot \sum_{i=1}^{A} \sum_{k=1}^{K} |20 \cdot \log p_{ik} - 20 \cdot \log r_{ik}|, \tag{1}$$

where i is the index of floorplans in either the training subset or the validation subset, k is the index of observation points within a floorplan, p_{ik} is the predicted value, and r_{ik} is the true value. The scattering plots of the training and validation subsets are shown in Figs. 6 (a) and (b), respectively. MAEs of 3.2 dB and 4.2 dB are achieved for the training subset and validation subset, respectively. These results are quite good compared with the results of the conventional empirical propagation models [21] that had an error of more than 10 dB. As shown in Fig. 6 (b), the prediction is uniformly distributed along the ideal line, implying that the model well predicts the E-field distribu-

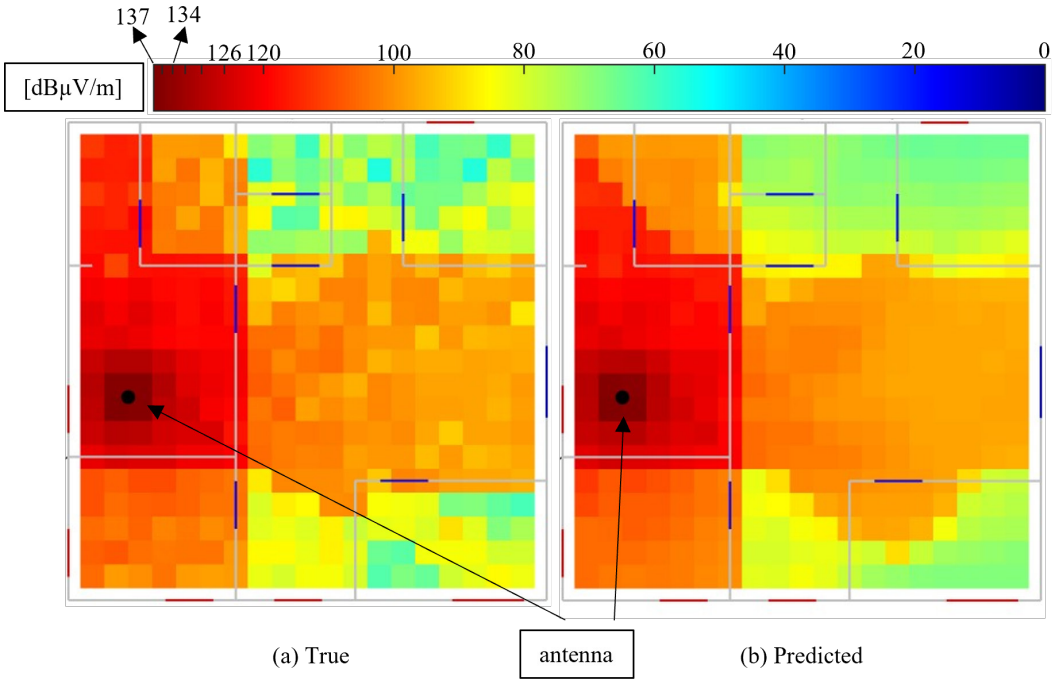

Fig. 7　Ground truth and result of prediction

tion in the floorplans of the validation subset. In other words, the model can "see" new floorplans that were never used during the model training process. Figures 7 (a) and (b) respectively depict the true and predicted E-field distributions in a selected data sample from the validation subset for comparison purposes. It is evident that the prediction model provides excellent results in regions with high strength values including line-of-sight regions and non-line-of-sight regions that are close to the Tx antenna. Meanwhile, the prediction model provides the results within 1 s, which is much faster than simulations that require 1.5 min with the option of GPU acceleration enabled.

4 Conclusion and Future Prospects

In this research, the author measured the EMF exposure level from a 28-GHz-band local 5G BS deployed on the campus of Tokyo Metropolitan University in Tokyo, Japan. It was found that the maximum E-field strength is not dependent on the traffic condition when the smartphone is powered on. Meanwhile, there is an increase of around 20 dB of the RMS E-field strength in cases with data traffic compared with cases of no traffic. 5G is paving its way, and many commercial BSs, including underground ones, will be newly deployed. The authors are currently investigating commercial 5G BSs. The author also developed an EMF exposure prediction model based on graph neural networks. The model can accurately and efficiently predict the EMF exposure level distribution in an indoor environment that is beyond the training subset. The author will explore the possibility of extending the model to outdoor scenarios in the future. In addition, the combining of measured data is also a promising direction for future exploration.

Acknowledgment

The author appreciates the support from the Ministry of Internal Affairs and Communications, Japan (JPMI10001) and the Tokyo Metropolitan University (TMU) local 5G research funding. The author thanks the support from Mr. Tsuchiya Naoto and Prof. Yukihisa Suzuki from TMU, and Mr. Kazuhiro Tobita from our research group.

References

1　T. Onishi, M. Ikuyo, K. Tobita, S. Liu, M. Taki, and S. Watanabe, "Radiofrequency Exposure Levels from Mobile Phone Base Stations in Outdoor Environments and an Underground Shopping Mall in Japan," Int. J. Environ. Res. Public Health, vol.18, no.15, p.8068, July 2021.
2　T. Onishi, K. Esaki, K. Tobita, M. Ikuyo, M. Taki and S. Watanabe, "Large-Area Monitoring of Radiofrequency Electromagnetic Field Exposure Levels from Mobile Phone Base Stations and Broadcast Transmission Towers by Car-Mounted Measurements around Tokyo," Electronics, vol.12, no.8, Feb. 2023.
3　MIC, https://en.go5g.go.jp/.
4　B. D. Van Veen, K. M. Buckley, "Beamforming: A versatile approach to spatial filtering," IEEE ASSP Magazine, vol.5, no.2, pp.4, 1988.
5　Ericsson, "Massive MIMO handbook 2022, " 2022.
6　S. Liu, T. Onishi, M. Taki, M. Ikuyo, K. Tobita, S. Watanabe, and Y. Suzuki,

"E-Field Strength Measurements of a 5G Base Station in 28 GHz Band for EMF Exposure Assessment," IEEE AP-S/URSI 2021, pp.49-50, Dec. 2021.
7 S. Liu, K. Tobita, T. Onishi, M. Taki, S. Watanabe, and Y. Suzuki, "In-Situ Measurement of EMF Exposure on a 28 GHz Band 5G Base Station," AT-AP-RASC 2022, May 2022.
8 S. Liu, T. Onishi, M. Taki, S. Watanabe, and Y. Suzuki, "EMF Exposure Measurements of 5G Base Stations Operating at 28 GHz Band in Japan," BioEM 2022, June 2022.
9 D. Colombi, F. Ghasemifard, P. Joshi, B. Xu, C. D. Paola, and C. Törnevik, "Methods and Practices for In Situ Measurements of RF EMF Exposure From 5G Millimeter Wave Base Stations," IEEE Trans. Electromagn. Compat., vol.64, no.6, pp.1986–1993, Dec. 2022.
10 L. Chiaraviglio *et al.*, "EMF Exposure in 5G Standalone mm-Wave Deployments: What Is the Impact of Downlink Traffic?," IEEE Open J. Commun. Soc., vol.3, pp.1445–1465, 2022.
11 S. Q. Wali, A. Sali, J. K. Allami, and A. F. Osman, "RF-EMF Exposure Measurement for 5G Over Mm-Wave Base Station with MIMO Antenna," IEEE Access, vol.10, pp.9048–9058, 2022.
12 J. Schuster, and R. Luebbers, "Comparison of site-specific radio propagation path loss predictions to measurements in an urban area," in Proc. IEEE Int. Symp. Antennas Propag. USNC-URSI Radio Sci. Meeting, pp.1210–1213, July 1996.
13 Karl S. Kunz, and Raymond J. Luebbers, "The Finite Difference Time Domain Method for Electromagnetics," CRC press, 1993.
14 G. E. Karniadakis, I. G. Kevrekidis, L. Lu, P. Perdikaris, S. Wang, and L. Yang, "Physics-informed machine learning," Nat. Rev. Phys., vol.3, no.6, pp.422–440, June 2021.
15 M. M. Bronstein, J. Bruna, Y. LeCun, A. Szlam, and P. Vandergheynst, "Geometric deep learning: going beyond euclidean data," IEEE Signal Process. Mag., vol.34, no.4, pp.18-42, July 2017.
16 S. Liu, N. Tsuchiya, T. Onishi, M. Taki, S. Watanabe, and Y. Suzuki, "Radiofrequency Exposure Measurements on a 28 GHz Band 5G Base Station," URSI GASS 2023, (accepted).
17 MIC, https://www.soumu.go.jp/main_content/000802944.pdf.
18 S. Liu, T. Onishi, M. Taki, and S. Watanabe, "A Generalizable Indoor Propagation Model Based on Graph Neural Networks," IEEE Trans. Antennas Propag., (accepted), doi: 10.1109/TAP.2023.3281061.
19 S. Liu, T. Onishi, M. Taki, and S. Watanabe, "A Graph Neural Network-Based Electric-Field Prediction Model for Exposure Assessments," IEEE AP-S/URSI 2023, (accepted).
20 F. Scarselli, M. Gori, A. C. Tsoi, M. Hagenbuchner, and G. Monfardini, "The graph neural network model," IEEE Trans. Neural Netw., vol.20, no.1, pp.61–80, Jan. 2009.
21 H. Hashemi, "The indoor radio propagation channel," Proc. IEEE, vol.81. no.7, pp.943–967, July 1993.

Liu Sen（りゅう しん）
電磁波研究所
電磁波標準研究センター
電磁環境研究室
研究員
博士（工学）
環境電磁工学
【受賞歴】
2021 年　アンテナ・伝播研究専門委員会若手奨励賞
2021 年　Young Scientist Award (URSI GASS 2021)
2021 年　IEEE AP-S Japan Young Engineer Award

大西 輝夫（おおにし てるお）
電磁波研究所
電磁波標準研究センター
電磁環境研究室
主任研究員
博士（工学）
環境電磁工学
【受賞歴】
2017 年　IEC 1906 賞
2010 年　経済産業省産業技術環境局長表彰
2010 年　日本 ITU 協会賞

多氣 昌生（たき まさお）
電磁波研究所
電磁波標準研究センター
電磁環境研究室
上席研究員／
東京都立大学
名誉教授
システムデザイン研究科
特任教授
工学博士
環境電磁工学
【受賞歴】
2020 年　第 70 回「電波の日」　総務大臣表彰
2018 年　電気学会　業績賞
2010 年　平成 22 年度工業標準化事業表彰　経済産業大臣賞

渡辺 聡一（わたなべ そういち）
電磁波研究所
電磁波標準研究センター
電磁環境研究室
室長
博士（工学）
環境電磁工学
【受賞歴】
2022 年　電波功績賞電波産業会会長表彰
2021 年　電子情報通信学会業績賞
2012 年　平成 24 年度文部科学大臣表彰　科学技術賞